Instrument design and characterization of the Millimeter Bolometer Array Camera on the Atacama Cosmology Telescope

D. S. Swetz[a], P. A. R. Ade[b], C. Allen[c], M. Amiri[d], J. W. Appel[e], E. S. Battistelli[o,d], B. Burger[d], J. A. Chervenak[c], A. J. Dahlen[e], S. Das[f], S. Denny[e], M. J. Devlin[a], S. R. Dicker[a], W. B. Doriese[g], R. Dünner[p,e], T. Essinger-Hileman[e], R. P. Fisher[e], J. W. Fowler[e], X. Gao[h], A. Hajian[f], M. Halpern[d], P. C. Hargrave[b], M. Hasselfield[d], G. C. Hilton[g], A. D. Hincks[e], K. D. Irwin[g], N. Jarosik[e], M. Kaul[a], J. Klein[a], S. Knotek[d], J. M. Lau[i], M. Limon[j], R. H. Lupton[f], T. A. Marriage[f], K. L. Martocci[k], P. Mauskopf[b], S. H. Moseley[c], C. B. Netterfield[l], M. D. Niemack[e], M. R. Nolta[m], L. Page[e], L. P. Parker[e], B. A. Reid[f], C. D. Reintsema[g], A. J. Sederberg[e], N. Sehgal[n], J. L. Sievers[m], D. N. Spergel[f], S. T. Staggs[e], O. R. Stryzak[e], E. R. Switzer[e], R. J. Thornton[a], C. Tucker[b], E. J. Wollack[c], Y. Zhao[e]

[a]University of Pennsylvania, Department of Physics and Astronomy, 209 S. 33rd St, Philadelphia, PA, 19104, USA;
[b]Cardiff University, Department of Physics and Astronomy, 5 The Parade, Cardiff, CF24 3AA, UK;
[c]Code 665, NASA/Goddard Space Flight Center, Greenbelt, MD 20771;
[d]University of British Columbia, Department of Physics and Astronomy, Vancouver, BC Canada V6T 1Z1;
[e]Princeton University, Department of Physics, Jadwin Hall, Princeton, NJ 08544-0708;
[f]Princeton University, Department of Astrophysical Sciences, Peyton Hall, Princeton, NJ 08544-1001;
[g]National Institute of Standards and Technology, 325 Broadway, Boulder, CO 80305;
[h]Royal Observatory, UK Astronomy Technology Centre, Blackford Hill, Edinburgh EH9 3HJ, UK;
[i]Stanford University Physics Department, 382 Via Pueblo Mall, Stanford, CA 94305;
[j]Columbia Astrophysics Laboratory, 550 W. 120th St. Mail Code 5247, New York, NY 10027;
[k]City University of New York, Department of Physics, 365 5th Avenue, Suite 6412, New York, NY 10016;
[l]University of Toronto, Department of Physics, 60 St. George Street, Toronto, ON M5S 1A7, Canada;
[m]University of Toronto, Canadian Institute for Theoretical Astrophysics, 60 St. George St, Toronto, ON Canada M5S 3H8;
[n]Rutgers University, Department of Physics and Astronomy, 136 Frelinghuysen Road Piscataway, NJ 08854;
[o]University of Rome "La Sapienza", Department of Physics, Piazzale Aldo Moro 5, I-00185 Rome, Italy;
[p]Pontificia Universidad Catlica de Chile, Departamento de Astronoma y Astrofsica, Facultad de Fsica, Casilla 306, Santiago 22, Chile

Further author information: (Send correspondence to Daniel S. Swetz)
Daniel S. Swetz: E-mail: swetz@sas.upenn.edu, Telephone: 1 215 573 7558

Millimeter and Submillimeter Detectors and Instrumentation for Astronomy IV
edited by William D. Duncan, Wayne S. Holland, Stafford Withington, Jonas Zmuidzinas
Proc. of SPIE Vol. 7020, 702008, (2008) · 0277-786X/08/$18 · doi: 10.1117/12.789876

ABSTRACT

The Millimeter Bolometer Array Camera (MBAC) was commissioned in the fall of 2007 on the new 6-meter Atacama Cosmology Telescope (ACT). The MBAC on the ACT will map the temperature anisotropies of the Cosmic Microwave Background (CMB) with arc-minute resolution. For this first observing season, the MBAC contained a diffraction-limited, 32 by 32 element, focal plane array of Transition Edge Sensor (TES) bolometers for observations at 145 GHz. This array was coupled to the telescope with a series of cold, refractive, reimaging optics. To meet the performance specifications, the MBAC employs four stages of cooling using closed-cycle ^{3}He/^{4}He sorption fridge systems in combination with pulse tube coolers. In this paper we present the design of the instrument and discuss its performance during the first observing season. Finally, we report on the status of the MBAC for the 2008 observing season, when the instrument will be upgraded to a total of three separate 1024-element arrays at 145 GHz, 220 GHz and 280 GHz.

Keywords: instrument design, cryogenics, receiver, pulse tube, CMB, bolometer, TES, array

1. INTRODUCTION

The Cosmic Microwave Background (CMB) is the remnant thermal radiation produced roughly 380,000 years after the Big Bang. Today, this nearly perfect black-body radiation is red-shifted to a temperature of ~ 2.7 K, with peak emission at $\lambda \sim 2$ mm. Studies of the temperature variations of the CMB sky have allowed us to learn much about the geometry, age, and contents of the universe.[1] When combined with other cosmological surveys, these data tightly constrain cosmological parameters, leading to a standard model of cosmology (for a recent survey, see Ref. 2). Most experiments have focused on measuring the anisotropy on large angular scales ($\theta \gtrsim 15$ arc-minutes), which are produced by density inhomogeneities in the early Universe. Anisotropies at smaller angular scales reflect the development of structure throughout the history of the Universe. One effect at small angular scales is the Sunyaev-Zel'dovich (SZ) effect. The SZ is spectral distortion of the CMB, caused by inverse-Compton scattering of CMB photons as they pass through hot gas in clusters of galaxies. Since the amplitude of the SZ effect is largely independent of redshift, galaxy clusters can be detected to high redshifts. Because of this feature, blind surveys may yield unbiased, mass-limited catalogues of galaxy cluster positions on the sky.[3] By combining SZ galaxy-cluster measurements with optical and X-ray data, the masses, temperatures, and redshifts of the clusters can be determined. The cluster density as a function of redshift will help map out the growth of structure in the universe, that in turn will constrain the dark energy equation of state.

The Atacama Cosmology Telescope (ACT) is a new 6-meter diameter telescope designed to make detailed measurements at millimeter wavelengths with arc-minute resolution. The construction of the ACT was completed in the summer of 2007. The telescope is located at a height of 5,190 meters in Atacama desert in the Chilean Andes. The primary science camera for the ACT is the Millimeter Bolometer Array Camera (MBAC). The MBAC is designed to make detailed measurements of the CMB temperature anisotropy at angular scales up to multipole $l \approx 10{,}000$. The MBAC will simultaneously observe in three frequency bands at 145 GHz, 220 GHz and 280 GHz, with bandwidths of approximately 30 GHz for each frequency. These frequency bands were chosen to probe the decrement, null, and increment of the SZ signal. Choosing the frequencies in this way allows one to separate the galaxy clusters from primary CMB anisotropy and other foreground contamination. We expect to detect hundreds of clusters of galaxies, which we will use to produce a mass-limited galaxy cluster catalogue.

The MBAC was deployed to the ACT site in September 2007. For this first observing season, it was outfitted with the 145 GHz array with a 1024-pixel array of Transition Edge Sensor (TES) bolometers.[4,5] Science observations began on 14 November and continued until 17 December. The camera was brought back to North America in January 2008 with the onset of the Bolivian winter. The two other arrays are currently being installed in preparation for a second observing season, with data analysis from the first observing season underway.

This paper is one of a series of papers in these proceedings which describe the technical aspects of the ACT: the detectors, the telescope, the cryogenic camera, and the data acquisition systems.[5,6,7,8,9] In this paper we give a description of the MBAC receiver. In Section 2 we focus on the mechanical design of the instrument. In Section 3 we describe the cryogenic system. In Section 4 we discuss the performance of the instrument, both in the lab and during this first observing season. In Section 5 we report on the current status and plans for the upcoming observing season before concluding in Section 6.

2. INSTRUMENT DESIGN

The MBAC is a cryogenic receiver for the ACT. All facets of the design had to meet the scientific goals and requirements of the ACT project.[10] The telescope observes by continuously moving the entire $\sim$ 40 metric ton upper structure of the telescope 10° peak to peak in azimuth at constant elevation with a constant velocity of up to 2°/second with a 400 ms turn around time.[6] The MBAC mates directly to the telescope, roughly on the rotation axis, and scans with it; all optical elements move together during the scan. With this scan strategy in mind, the MBAC was designed to be extremely rigid while remaining as lightweight as possible.

2.1 Cryostat Mechanical Design

The vacuum shell is a cylinder measuring 0.94 meters diameter and 1.22 meters long made out of 6.35 mm thick aluminum. This shape was chosen because it is relatively easy to manufacture, fits in the allocated space, and has good strength to weight ratio. The shell diameter was dictated by the area of the focal plane, and the length by the cold optics that were needed to reimage the focus of the off-axis Gregorian ACT telescope. A cut away of the MBAC highlighting major internal components is shown in Figure 1. Due to the large size of the shell, we chose aluminum to keep the weight as low as possible. The front and back of the vacuum-shell cylinder are 25.4 mm thick aluminum plates. The MBAC is mounted to the ACT at the flange that joins the front plate to the vacuum cylinder, providing an extremely rigid plane that can be precisely aligned with the optical axis of the telescope. This plane was used as the base for all optical elements inside the MBAC, ensuring that the alignment was independent of variations in the vacuum shell caused by pressure and temperature. The front plate has two additional aluminum plates attached by G10 cylinders. The first plate ("40K plate") is cooled to $\sim$ 40 K. The second plate ("4K plate"), which is attached to the 40K plate, is cooled to $\sim$ 4 K. These two plates each have a large radiation shield attached to them. The shields are nested so that the outermost one completely surrounds the inner one. The helium fridges and optics tubes are rigidly mounted to the 4K plate, and are located between the 4K plate and its corresponding radiation shield. The vacuum shell is split about 200 mm back from the front plate. This serves to decouple the pulse tube fridges from the rest of the system, thus exposing the cold plates, optics, and detectors (see Figure 2). All of the cabling for the thermometry, detectors, and the detector readout comes in through ports in the front vacuum shell section. These cables are heat sunk at both the 40K and at 4K plates. An advantage of this design is that it allows for access to all of the cabling without making or breaking any cable attachments.

The G10 cylinders that connect the two plates to the front plate create a robust mechanical connection between the optics and front plate. Once the cryostat is bolted into the telescope receiver cabin, a laser tracker* is used to locate the front plate in relation to the primary mirror, translating the position of the internal cold optics to the rest of the telescope system.[6] The cryostat is attached to the telescope receiver cabin on a mount that has three dimensional adjustment. This system provides a way to accurately align the cold optics to the telescope and enables the optics to move in concert with the telescope as it scans. Figure 3 shows the mating of MBAC in the receiver cabin and its relation to the primary and secondary mirrors of the ACT.

2.2 Detectors and Readout Electronics

The MBAC houses three 1024-element arrays of TES bolometer detectors that lie side by side at the reimaged focal plane of the ACT. Each array consists of 32 individually stacked columns, with each column consisting of 32 elements. The array elements are close-packed with no feed horns, filling the ACT focal plane. The arrays are cooled to 300 mK and then biased onto their transitions. The individual bolometers are read out in a time-multiplexed fashion through SQUID multiplexers that are controlled and read out by the Multi-Channel Electronics (MCE). For details on the TES bolometers, array construction, and characterization see Ref. 4 and Ref. 5. Details of the MCE readout electronics can be found in Ref. 8 and Ref 11. The SQUID amplifiers are sensitive to changes in magnetic fields. To reduce this signal, we have incorporated three layers of cryoperm magnetic shielding into the optics tubes of each array. Details of the magnetic shielding can be found in Ref. 7.

*Laser tracker manufactured by Faro. For more information see www.faro.com

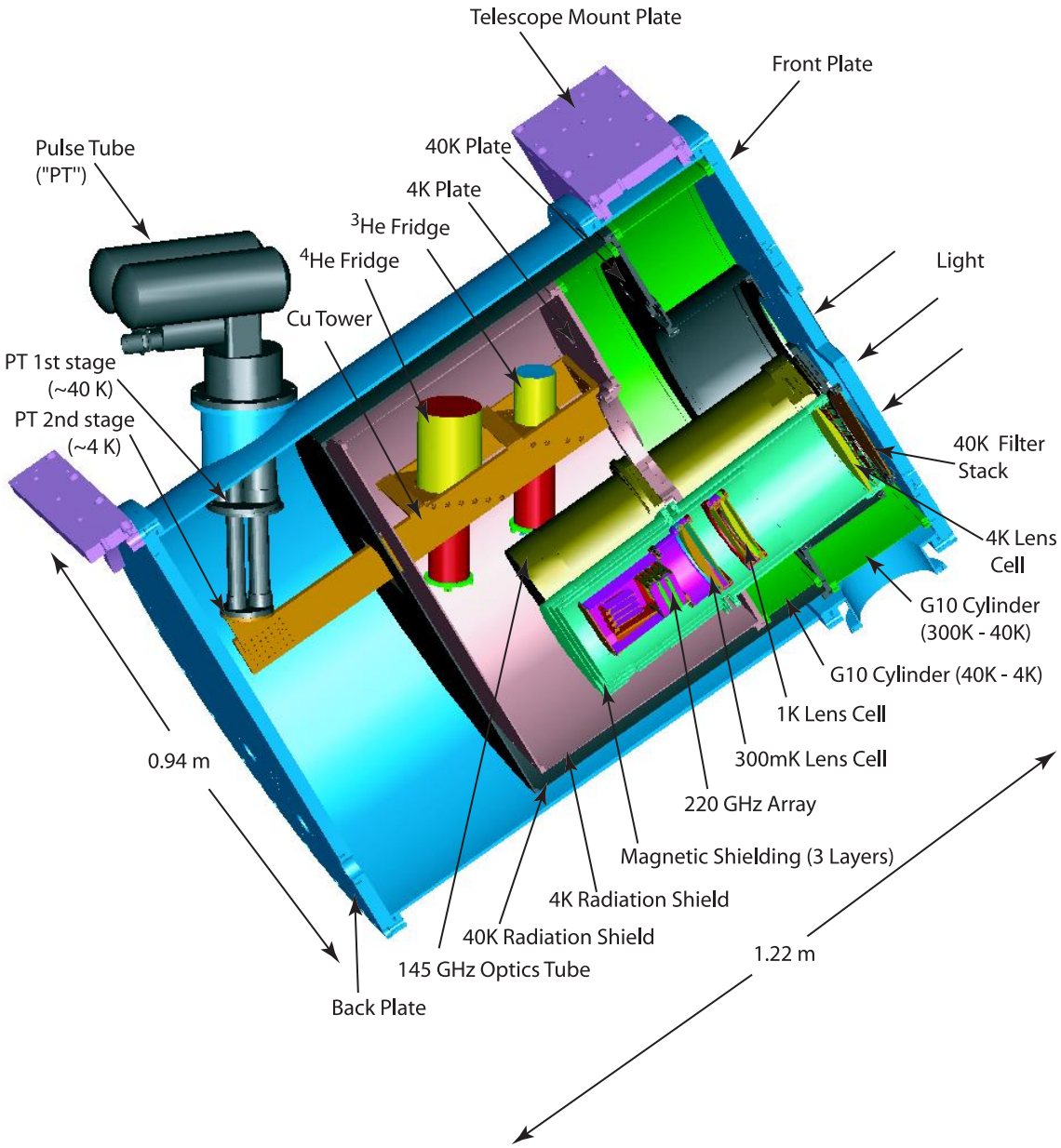

Figure 1. Cut away of the MBAC cryostat showing the location of the internal components. A cut away of the 220 GHz optics tube is also shown, giving the location of its lenses, filters, and array, which is similar for all three tubes. The 280 GHz optics tube mounts just above the 145 and 220 GHz optics tubes, but is removed for clarity. The connection of the first stage of the pulse tube and its radiation shielding to the 40K plate is also omitted for clarity.

Figure 2. Left Panel: Picture of the MBAC open. The vacuum shell, pulse tubes and the two radiation shields have been removed, exposing the large (4600 cm^2) 4K plate. The three sorption fridges (G10 cylinders inclined at $\sim 45^\circ$) are mounted on the two vertical copper bars which in turn are attached to the 4K plate. The cryoperm magnetic shield (silver vertical cylinder) surrounds the 145 GHz optics tube which is rigidly attached to the 4K plate.[7] Right Panel: Picture of the MBAC closed. The receiver is shown at the approximate observing angle at which it is mounted on the telescope. The pulse tubes are mounted in the MBAC so that they are close to horizontal during normal operation. Light enters the cryostat through the three rectangular windows located between the handles that are removed during observations. The 145 GHz UHMWPE window is installed (lower-right window) (see Sec. 2.4). The total volume is 700 liters and the total mass is 530 kg. The MCE readout electronics are bolted to the vacuum shell through a mounting plate, forming a RF seal.

2.3 Optics

The ACT's primary and secondary mirrors are in an off-axis, aplanatic Gregorian configuration. The internal reimaging optics consists of a series of separate refractive lenses and filters for each of the three frequency bands.[12] To minimize its size, the MBAC is aligned near the optical axis of the telescope. As the ACT is an off-axis Gregorian, the optimal focal plane is not perpendicular to the optical axis, and because the Gregorian focal plane is not telecentric, the lenses must be held at compound angles inside the cryostat. Furthermore, because each array has a separate optical path, the optical elements for each array must be closely packed to maximize sky overlap.[7] Each array's lens system consists of three silicon lenses, shown in Figure 4. A series of capacitive mesh low-pass filters along with a band defining filter are used to define the frequency band of each detector array. In order to keep the optical loading on the detectors to a minimum, the final band-pass filter is cooled to $\approx$ 300 mK . The placement of the final lens with respect to the array has the tightest tolerance of all optical elements and so it is attached directly to the array mounting assembly and also cooled to $\approx$ 300 mK. Behind the band-pass filter, the array is enclosed in a 300 mK cavity which is painted with a stycast and lampblack coating to absorb stray light. An image of the primary is formed along the optical path internal to the MBAC, where a cold aperture stop (Lyot stop) is placed and held at $\approx$ 1 K. While the actual temperatures of the remaining optical elements are not critical, they are cooled in stages to limit the loading on the fridges.

2.4 Vacuum Windows

One challenge posed by the optical design was building a vacuum window that would accommodate all three arrays simultaneously. The vacuum window was placed near the Gregorian focus of the telescope to minimize

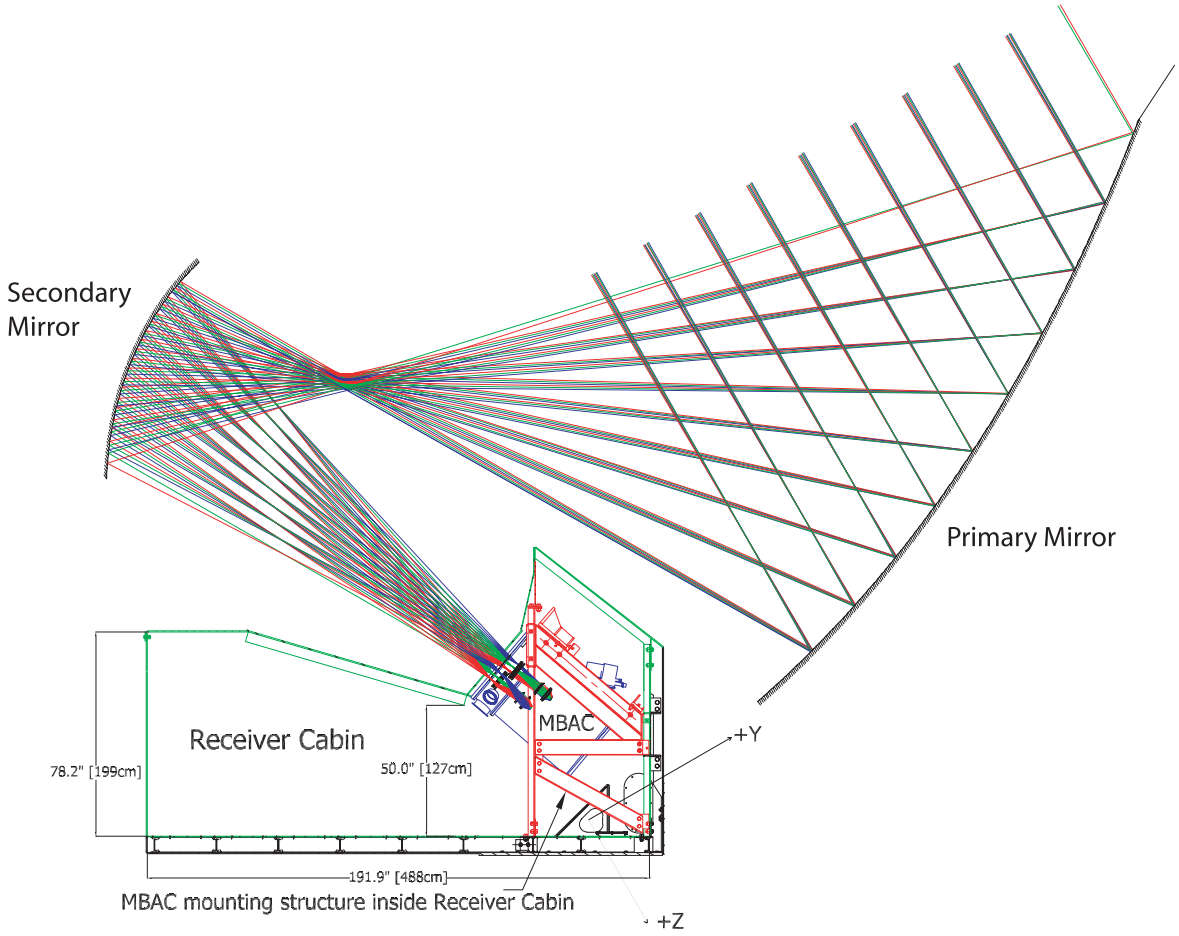

Figure 3. The MBAC mounted in the receiver cabin of the telescope. The receiver and telescope were designed to work together. The width of the receiver cabin is ≈ 4 meters. The MBAC enters though doors on the front of the receiver cabin (left side of figure), and passes through the MBAC mounting structure whose width is ≈ 1 meter where it is then hoisted and bolted into place. The MBAC mounting structure allows for positioning of the MBAC, aligning the internal optics to the primary mirror. The entire telescope structure, primary, secondary, receiver cabin, and the MBAC, move together.

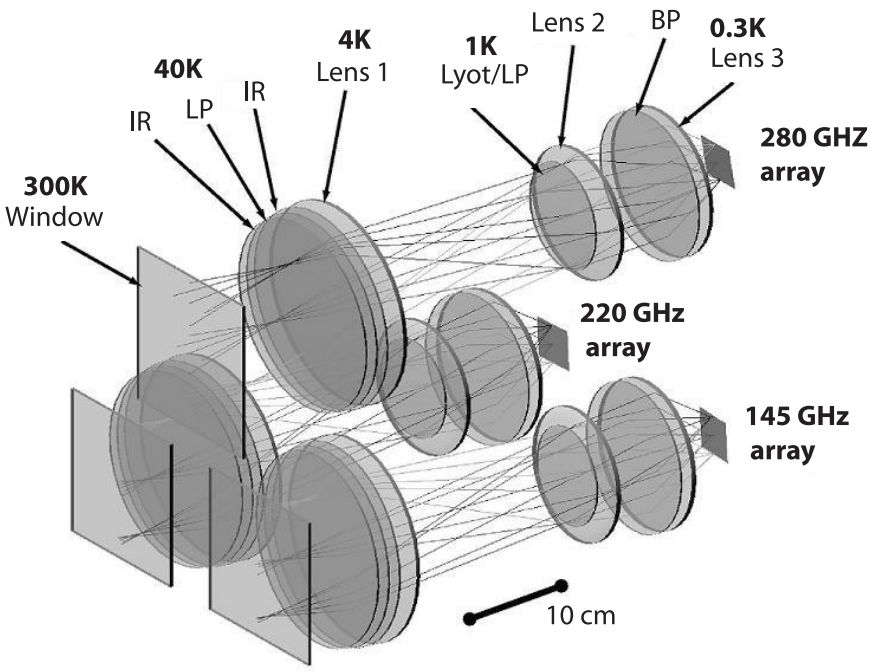

Figure 4. Three dimensional model of the cold reimaging optics for the MBAC. The optical elements for each array are separated into individual optics tubes. Each array has a similar set of optical elements. The 280 GHz elements and temperatures are labeled. The lenses are labeled Lens 1 to 3, with lens one being closest to the 300 K window. The low-pass capacitive mesh filters are labeled LP and the band-pass filter as BP. Infrared blocking filters labeled IR are shown for the 40 K stage only. Two other IR blocking filters, at 300 K and 4 K, are not shown along with a LP filter at 4 K and second LP filter at 1 K. The temperature of the components decrease moving toward the arrays to reduce the loading, with the band-pass filter, Lens 3, and arrays all held at 0.3 K

the size of the window and reduce the radiative load entering the cryostat. Even at this position, the smallest single window which encircled the beams for all three arrays was over 50 cm in diameter. At this size making a single large window becomes difficult. Another problem with a single large window is in the application of an anti-reflective (AR) coating. The optimal thickness to minimize reflections is $\lambda/2n$ while an AR layer of thickness $\lambda/4n$ gives maximum reflections; therefore a single thickness AR coating is not possible for all three of the ACT wavelength bands. Additionally, to maximize their sky overlap the three arrays are closely spaced. To accommodate these demands, three separate rectangular vacuum windows were chosen. This takes advantage of the image shape of the array at the window (shown in Figure 2 and Figure 4). The drawback to a rectangular window is that the stress is not uniformly distributed along the circumference, as in a circular window, but instead is concentrated in the corners. A number of window materials were considered. Thin window materials ($\sim$ 200 μm thick), such as mylar and kapton, have several disadvantages. First, they are fragile $-$ the chance of an accidental breakage is considerable. Second, in general, they consist of polar organic molecules that have strong absorbances near 2 mm. This would pose a problem for our longest wavelength band. Third, they typically have high refractive indexes that increase reflections and reduce transmission. Thick window materials ($\sim$ 20 mm thick) such as Zotefoam also have several disadvantages for us. The thickness of the pieces made them difficult to mount given the close spacing of the beams. The material also deforms considerably along the beam axis when the cryostat is evacuated. Therefore, we considered medium thickness materials ($\sim$ 4-9 mm). We choose to use 4 mm thick Ultra High Molecular Weight Polyethylene (UHMWPE) as the window material. Each window has an individually tuned expanded-teflon AR coatings. UHMWPE is an ideal material, as it is extremely strong and has low absorption at millimeter wavelengths. Measurements of the MBAC windows using

a Fourier transform spectrometer show transmissions of over 95% for the 145 GHz and 220 GHz bands and over 93% in the 280 GHz band.

3. CRYOGENICS AND THERMAL DESIGN

The cryogenic design was dictated by many requirements. The site location prevented the use of liquid cryogens; the optics design required multiple stages of cooling to reduce detector loading; the three detector arrays needed to be maintained at 300 mK continuously for over 18 hours, and recycle with in 6 hours. The ACT observes from sunset to sunrise; daytime observations are not possible because solar heating of the telescope causes deformation of the telescope structure significantly reducing the ~ 30 μm rms of the primary mirror.[6] The cryogenics also had to be able to perform stably when the telescope is scanning. In order to meet these requirements, the MBAC incorporates a series of different types of cooling mechanisms including pulse tube cryocoolers, closed-cycle ^{4}He sorption refrigerators, and a closed-cycle ^{3}He sorption refrigerator.

The primary cooling is achieved using two pulse tube cryocoolers[†]. The pulse tubes provide the first two stages of cooling, a 45 K first stage at a loading of 40 Watts and a 4.2 K second stage at 1 Watt. The next stage of cooling is accomplished using in-house built closed-cycle ^{4}He sorption refrigerators.[13,14] The sorption fridges were measured to have ~ 80 Joules cooling capacity and base temperatures of ~ 670 mK. The final stage of cooling is accomplished using a in-house built ^{3}He sorption fridge.[13] A separate ^{4}He fridge is used to precool and back the ^{3}He fridge. The ^{3}He fridge was measured to have 5.8 Joules cooling capacity and a base temperature of 240 mK. In order to meet the hold-time requirements, a detailed thermal model for each temperature stage was made. Table 1 lists the calculated loading, temperatures, and hold times for each of the four stages with all three optics tubes and arrays installed.

A schematic of the different thermal connections in the cryostat is shown in Figure 5. The pulse tubes and sorption fridges are thermally arranged to provide two cold temperature stages. In the first system, the pulse tube ("PT 1") is connected to the condenser plate of the ^{4}He backing fridge, condensing the high pressure helium gas in the fridge into liquid helium-4 in the evaporator. The charcoal sorption pump for ^{4}He backing fridge is then cooled, pumping on the liquid and providing a cold evaporator plate. The evaporator plate for the ^{4}He backing fridge is connected to the condensing plate of the ^{3}He fridge, providing the cooling necessary for the ^{3}He gas to condense into liquid onto its evaporator, which is pumped on in a similar way. The ^{3}He evaporator is finally connected to the 0.3 K lenses and filters ("lens cell") along with the detector arrays. The second pulse tube ("PT 2") is connected to the ^{4}He optics fridge, and is cooled in the same way as the other ^{4}He fridge. The evaporator for the ^{4}He optics fridge is connected to the 1 K lens cells. Arranging the fridges in this way has several advantages. Using a separate dedicated ^{4}He backing fridge provides more complete condensation of the ^{3}He gas, ensuring we get efficient recycling of the ^{3}He fridge. After the ^{3}He fridge is recycled, the ^{4}He backing-fridge has enough capacity to stay cold for the duration of the ^{3}He hold time, reducing the overall parasitic load on the ^{3}He fridge and allowing for longer hold times and lower base temperatures at 300 mK. Having two separate pulse tube/sorption fridge systems also allows us to thermally recycle the fridge systems faster than with one.

The system is cold until the liquid helium supply in the evaporator pots is exhausted. After this point, the charcoal is heated, releasing the gas and the condensing process is repeated. The recycling procedure is completely automated and can be controlled remotely. The total recycle time for all three sorption fridges is ~ 5.5 hours. Over the course of a night, the ^{3}He fridge can have small temperature drifts. To prevent these drifts from affecting the detectors, we thermally regulate the temperature of each detector stage independently.[9]

The two fridge assemblies are mounted into the cyrostat on separate copper towers (Figure 2). These copper towers provide a rigid mechanical mount for the sorption fridges and also provide high thermal conductivity from the sorption fridges to the pulse tubes. The base of a copper tower is bolted to the 4K plate, making the whole system mechanically robust enough to withstand the scanning motion of the telescope.

Several issues can arise when using pulse tube coolers. The pulse tube pulses at a frequency of 1.4 Hz, producing a 100 mK sine-wave temperature variation and inducing a mechanical vibration, both at the pulse

[†]Model PT-410 cryorefrigerator from Cryomech. For more information see www.cryomech.com

Table 1. Cooling capacity, calculated loading, and expected hold times for the four MBAC temperature stages with all three optics tubes installed. Calculated loading is based on a thermal model. Temperatures and hold times are predicted from measured load curves on the different fridges. Temperature increase with increased load, dT/dP, is obtained by making a linear approximation to a load curve in the loading region of interest. Temperature of the pulse tube is based on laboratory performance. Hold times and loading for the 1 K and 0.3 K stage use an elevated pulse tube second stage temperature. See Section 4 for details.

Temperature Stage	Fridge Capacity	Calculated Load	Temperature	dT/dP	Hold time
Pulse Tubes 1st stage	80 Watts @ 40 K	30 W	35 K	-	Continuous
Pulse Tubes 2nd stage	2 Watts @ 4.2K	0.16 W	3.2 K	1.4 K/W	Continuous
1 K Optics	78 Joules	670 μW	810 mK	0.12 mK/μW	32 hours
0.3 K Optics/Detectors	5.8 Joules	28 μW	285 mK	1.3 mK/μW	58 hours

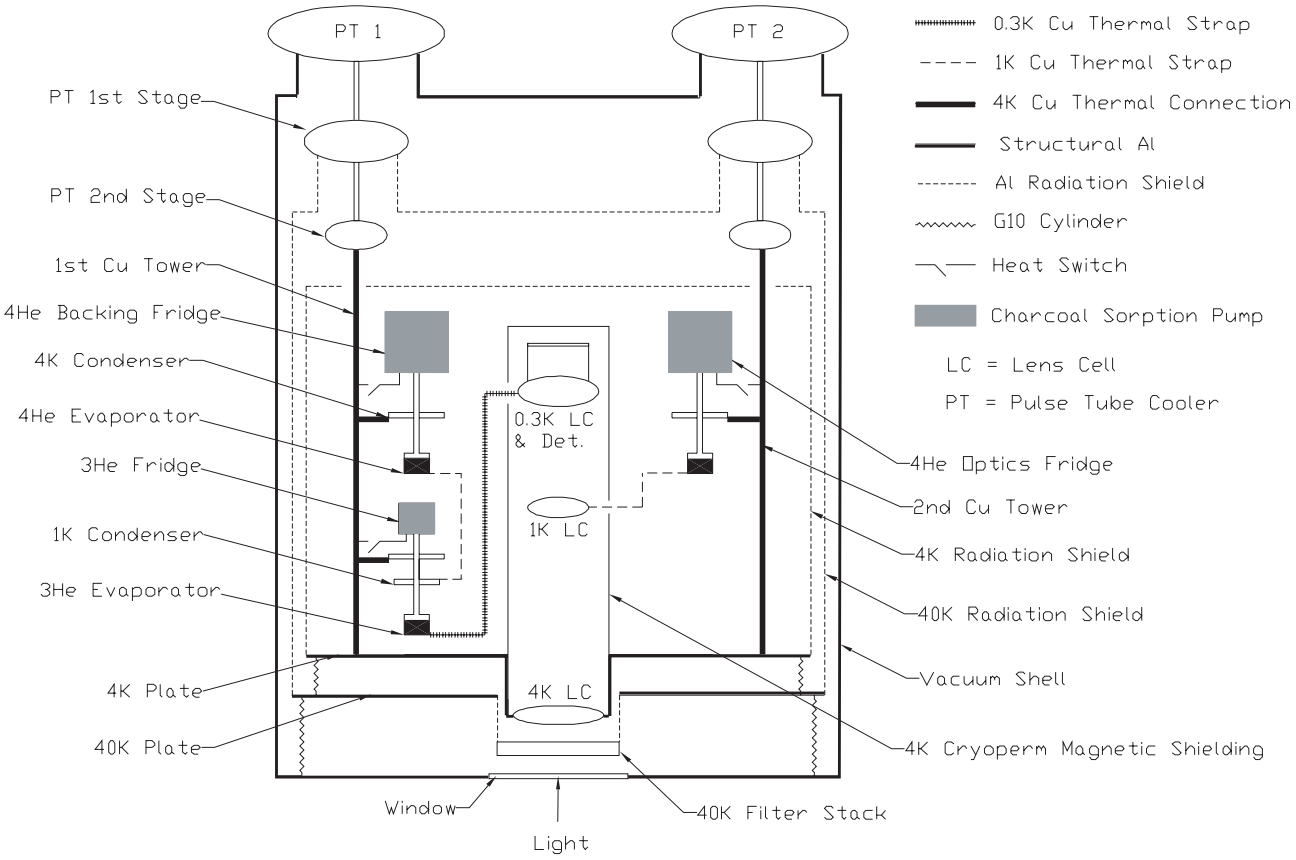

Figure 5. Schematic of the radiation shielding and thermal connections in the MBAC. Only a single optics tube is shown, but all are connected in a similar way and in parallel.

frequency. To limit the mechanical coupling of the pulse frequency, several strands of copper rope are used to attach the pulse tube cryocoolers to the copper towers. The heat capacity associated with the pumped helium of the sorption fridges damps out the thermal oscillation, preventing the signal from entering either the 300 mK stage or 1 K stage. Furthermore, the connection between the copper towers and the 4K cold plate has a low thermal conductance, acting as a low-pass filter on the temperature variations of the pulse tube. We have not seen the pulse tube oscillations in any of the lens cell temperature stages, nor in the detector data.

4. INSTRUMENT CHARACTERIZATION

Prior to deployment, several tests on the MBAC receiver were performed. One of these tests was to measure the strength of the system of stacked G10 cylinders. We calculated the total mass connected to the 4K plate to be $\sim$ 120 kg providing 11 N-m torque at the center of mass and observing angle on the telescope. We estimated the telescope acceleration at 0.3 g, increasing the estimated torque on the system to 14 N-m. To test the G10 strength, we hung 180 kg off of the 4K plate at a more severe moment arm, imparting 22 N-m torque onto the two stacked G10 cylinders. There was an initial deflection of 280 μm, but no sign of buckling of the cylinders was observed. To test for creep, we left the mass connected and continued to monitor the deflection. After two days, there was in increase of only 20 μm, at which point the deflection stopped increasing. We concluded that the stacked G10 cylinders were strong enough to withstand the telescope scan motion and would provide a very stable and rigid system for mounting the optics and helium sorption fridges. After installation of the MBAC on the telescope, we saw no signal of the telescope's scan pattern in the cryogenic data.

In order to operate at maximum capacity, pulse tube coolers and He sorption fridges must remain close to vertical. The ACT primarily scans at a constant elevation of 50.5°, but must be able to look at known sources such as planets for calibration and pointing purposes. We wanted the cryogenic system to perform through the entire range of telescope motion, 60° to 32° elevation, and so the fridges were designed to be mounted so that they were kept vertical when the telescope was pointed near the middle of its range, at 45° elevation. Cryogenic tests were performed with the MBAC held at both 60° and 30°. At these angles, there was little reduction in the performance of the pulse tube coolers. We did measure a small reduction in the cooling ability of the ^{3}He fridge of $\sim$ 0.1 mK/μW, along with a 8% reduction in total fridge capacity if the fridges were recycled at angles of 60° and 30°. The effects are relatively small and the MBAC is able to move through the entire elevation range of the ACT with minimal change in the cryogenic performance.

A series of hold time and load curve tests were performed to verify the thermal model predictions for the three sorption fridges. In the lab, we measured an 82 hour hold time for the ^{4}He optics fridge and a 48 hour hold time for the ^{3}He fridge with a single optics tube installed, which matched the thermal model prediction to 10%. With the MBAC on the telescope a similar series of tests were performed to verify that the system is on track to meet the cryogenic needs with all three sets of optics installed. In the first observing season we did not optimally heat sink the wires going to the array from the 4K plate. The added load from these wires reduced the hold time of the ^{3}He fridge to $\approx$ 20 hours on the telescope. This did not affect the performance of the instrument during this first season, but posed a problem for operation with all three arrays. To reduce the load on the 0.3 K stage from these wires, we have heat sunk the wires going to the array to 1 K. This should increase the hold time of the 0.3 K stage to over 50 hours with all three tubes installed. The numbers given in Table 1 are with the wires heat sunk in this way.

5. CURRENT STATUS AND PLANS

The MBAC was brought back from Chile in January 2007 after the first season of observations were complete. The 220 GHz and 280 GHz optics tubes have been installed along with the 220 GHz array. Cryogenic tests of the three tube system along with dark tests of both the 220 GHz and 145 GHz arrays have been successfully completed in the MBAC. The 280 GHz array is currently being assembled, and is due to be completed in early summer. A full light test of the two full arrays, along with a partially complete third array has been performed. We are on schedule to return to the site in early June 2008 and begin observations shortly thereafter.

6. CONCLUSIONS

We have designed and built the cryogenic receiver MBAC to work with the new Atacama Cosmology Telescope, taking into account the many design challenges imposed by the requirements of the ACT project. The MBAC houses three TES bolometer arrays, at 145, 220 and 280 GHz, and provides rigid mounting for the corresponding optical elements. It cools the optics and the arrays to the desired temperatures without the use of liquid cryogens using a series of mechanical pulse tube coolers and closed-cycle ^{4}He and ^{3}He sorption fridges. It has been installed on the ACT with the 145 GHz array and a first season of observations has been completed. The data analysis from this season, while still preliminary, indicates that the camera and receiver have worked well. We are preparing for a second observing season to begin in July 2008 with the three detector arrays installed.

ACKNOWLEDGMENTS

The MBAC team and the ACT collaboration would like to thank the many efforts of the Penn and Princeton Machine Shops, for the quality workmanship delivered in a timely manner often on short notice. We thank Danica Marsden for her help with the assembly and installation of the second and third optics tubes. We appreciate the help of Mike Mclaren for the many late nights he stayed to help close up the MBAC and help with packing. We would also like to thank Joe Cosco and Nigel Bennet of Cryomech for the helpful discussions regarding pulse tube coolers and their compressors.

This work was supported by the U.S. National Science Foundation through awards AST-0408698 for the ACT project. Funding was also provided by the University of Pennsylvania and Princeton University.

REFERENCES

[1] Dunkley, J., Komatsu, E., Nolta, M. R., Spergel, D. N., Larson, D., Hinshaw, G., Page, L., Bennett, C. L., Gold, B., Jarosik, N., Weiland, J. L., Halpern, M., Hill, R. S., Kogut, A., Limon, M., Meyer, S. S., Tucker, G. S., Wollack, E., and Wright, E. L., "Five-Year Wilkinson Microwave Anisotropy Probe (WMAP) Observations: Likelihoods and Parameters from the WMAP data," *ArXiv e-prints* **803**, arXiv:0803.0586 (2008).

[2] Komatsu, E., Dunkley, J., Nolta, M. R., Bennett, C. L., Gold, B., Hinshaw, G., Jarosik, N., Larson, D., Limon, M., Page, L., Spergel, D. N., Halpern, M., Hill, R. S., Kogut, A., Meyer, S. S., Tucker, G. S., Weiland, J. L., Wollack, E., and Wright, E. L., "Five-Year Wilkinson Microwave Anisotropy Probe (WMAP) Observations: Cosmological Interpretation," *ArXiv e-prints* **803**, arXiv:0803.0547 (2008).

[3] Carlstrom, J. E., Holder, G. P., and Reese, E. D., "Cosmology with the Sunyaev-Zel'dovich Effect," *Ann. Rev. Astrophys.* **40**, 643–680 (2002).

[4] Niemack, M. D., Zhao, Y., Wollack, E., Thornton, R., Switzer, E. R., Swetz, D. S., Staggs, S. T., Page, L., Stryzak, O., Moseley, H., Marriage, T. A., Limon, M., Lau, J. M., Klein, J., Kaul, M., Jarosik, N., Irwin, K. D., Hincks, A. D., Hilton, G. C., Halpern, M., Fowler, J. W., Fisher, R. P., Dünner, R., Doriese, W. B., Dicker, S. R., Devlin, M. J., Chervenak, J., Burger, B., Battistelli, E. S., Appel, J., Amiri, M., Allen, C., and Aboobaker, A. M., "A kilopixel array of TES bolometers for ACT: Development, testing, and first light," *J. Low Temp. Phys.* **151**(3-4), 690–696 (2008).

[5] Zhao, Y., Allen, C., Amiri, M., Appel, J. W., Battistelli, E. S., Burger, B., Chervenak, J. A., Dahlen, A., Denny, S., Devlin, M. J., Dicker, S. R., Doriese, W. B., Dünner, R., Essinger-Hileman, T., Fisher, R. P., Fowler, J. W., Halpern, M., Hilton, G. C., Hincks, A. D., Irwin, K. D., Jarosik, N., Klein, J., Lau, J. M., Marriage, T. A., Martocci, K., Moseley, H., Niemack, M. D., Page, L., Parker, L. P., Sederberg, A., Staggs, S. T., Stryzak, O. R., Swetz, D. S., Switzer, E. R., Thornton, R. J., and Wollack, E. J., "Characterization of transition edge sensors for the Millimeter Bolometer Array Camera on the Atacama Cosmology Telescope," *Also in these Proc. SPIE* .

[6] Hincks, A. D., Ade, P. A. R., Allen, C., Amiri, M., Appel, J. W., Burger, E. S. B. A., Chervenak, J. A., Dahlen, A. J., Denny, S., Devlin, M. J., Dicker, S. R., Doriese, W. B., Dünner, R., Essinger-Hileman, T., Fisher, R. P., Fowler, J. W., Halpern, M., C.Hargrave, P., Hasselfield, M., Hilton, G. C., Irwin, K. D., Jarosik, N., Kaul, M., Klein, J., Lau, J. M., Limon, M., Lupton, R. H., Marriage, T. A., Martocci, K. L., Mauskopf, P., Moseley, S. H., Netterfield, C. B., Niemack, M. D., Nolta, M. R., Page, L., Parker, L. P.,

Sederberg, A. J., Staggs, S. T., Stryzak, O. R., Swetz, D. S., Switzer, E. R., Thornton, R. J., Tucker, C., Wollack, E. J., and Zhao, Y., "The effects of the mechanical performance and alignment of the Atacama Cosmology Telescope on the sensitivity of microwave observations," *Also in these Proc. SPIE* .

[7] Thornton, R. J., Ade, P. A. R., Allen, C., Amiri, M., Appel, J., Battistelli, E. S., Burger, B., Chervenak, J., Devlin, M. J., Dicker, S. R., Doriese, W. B., Essinger-Hileman, T., Fisher, R. P., Fowler, J. W., Halpern, M., Hargrave, P. C., Hasselfield, M., Hilton, G. C., Hincks, A. D., Irwin, K. D., Jarosik, N., Kaul, M., Klein, J., Lau, J. M., Limon, M., Marriage, T. A., Martocci, K., Mauskopf, P., Moseley, H., Niemack, M. D., Page, L., Parker, L. P., Reidel, J., Reintsema, C. D., Staggs, S. T., Stryzak, O. R., Swetz, D. S., Switzer, E. R., Tucker, C., Wollack, E. J., and Zhao, Y., "Optomechanical design and performance of a compact three-frequency camera for the MBAC receiver on the Atacama Cosmology Telescope," *Also in these Proc. SPIE* .

[8] Battistelli, E. S., Amiri, M., Burger, B., Devlin, M. J., Dicker, S. R., Doriese, W. B., D"unner, R., Fisher, R. P., Fowler, J. W., Halpern, M., Hasselfield, M., Hilton, G. C., Hincks, A. D., Irwin, K. D., Kaul, M., Klein, J., Knotek, S., Lau, J. M., Limon, M., Marriage, T. A., Niemack, M. D., Page, L., Reintsema, C. D., Staggs, S. T., Swetz, D. S., Switzer, E. R., Thornton, R. J., and Zhao, Y., "Automated SQUID tuning procedure for kilopixel arrays of TES bolometers on ACT," *Also in these Proc. SPIE* .

[9] Switzer, E. R., Allen, C., Amiri, M., Appel, J., Battistelli, E. S., Burger, B., Chervenak, J., Dahlen, A., Das, S., Devlin, M. J., Dicker, S. R., Doriese, W. B., Dünner, R., Essinger-Hileman, T., Fisher, R. P., Gao, J. W. F. X., Halpern, M., Hasselfield, M., Hilton, G. C., Hincks, A. D., Irwin, K. D., Jarosik, N., Kaul, M., Knotek, S., Klein, J., Lau, J. M., Limon, M., Lupton, R., Marriage, T. A., Martocci, K., Moseley, H., Netterfield, B., Niemack, M. D., Nolta, M., Page, L., Parker, L., Reid, B., Reintsema, C. D., Sederberg, A., Sievers, J., Spergel, D., Staggs, S. T., Stryzak, O., Swetz, D. S., Thornton, R., Wollack, E., and Zhao, Y., "System and control software for the Atacama Cosmology Telescope," *Also in these Proc. SPIE* .

[10] Fowler, J. W., "The Atacama Cosmology Telescope Project," *Proc. SPIE* **5498**, 1–10 (2004).

[11] Battistelli, E. S., Amiri, M., Burger, B., Halpern, M., Knotek, S., Ellis, M., Gao, X., Kelly, D., MacIntosh, M., Irwin, K., and Reintsema, C., "Functional description of read-out electronics for time-domain multiplexed bolometers for millimeter and sub-millimeter astronomy," *J. Low Temp. Phys.* **151**(3-4), 908–914 (2008).

[12] Fowler, J. W., Niemack, M. D., Dicker, S. R., Aboobaker, A. M., Ade, P. A. R., Battistelli, E. S., Devlin, M. J., Fisher, R. P., Halpern, M., Hargrave, P. C., Hincks, A. D., Kaul, M., Klein, J., Lau, J. M., Limon, M., Marriage, T. A., Mauskopf, P. D., Page, L., Staggs, S. T., Swetz, D. S., Switzer, E. R., Thornton, R. J., and Tucker, C. E., "Optical design of the Atacama Cosmology Telescope and the Millimeter Bolometric Array Camera," *Appl. Opt.* **46**(17), 3444–3454 (2007).

[13] Devlin, M. J., Dicker, S. R., Klein, J., and Supanich, M. P., "A high capacity completely closed-cycle 250 mk ^{3}He refrigeration system based on a pulse tube cooler," *Cryogenics* **44**, 611–616 (2004).

[14] Lau, J., Benna, M., Devlin, M., Dicker, S., and Page, L., "Experimental tests and modeling of the optimal orifice size for a closed cycle ^{4}He sorption refridgerator," *Cryogenics* **46**, 809–814 (2006).